Comparison of modified boehmite nanoplatelets and nanowires for dye removal from aqueous solution

Mojtaba Kamari[a], Saber Shafiee[a], Farhad Salimi[a,*], Changiz Karami[b]

[a]*Department of chemical engineering, Kermanshah Branch, Islamic Azad University, Kermanshah, Iran,
emails: f.salimi@iauksh.ac.ir (F. Salimi), Mirzamojtaba10@gmail.com (M. Kamari), saber_s_al2@yahoo.com (S. Shafiee)*
[b]*Nano Drug Delivery Research Center, Kermanshah University of Medical Sciences, Kermanshah, Iran, email: changiz.karami@gmail.com*

ABSTRACT

In this study, boehmite (–AlOOH) nanoplatelets and nanowires were synthesized at a pH of 5 and 12, respectively, modified with sulfonic acid (–AlOOH-SA5), (–AlOOH-SA12), and were used to adsorb eriochrome black T (EbT) dye solutions. Transmission electron microscopy, scanning electron microscopy, Fourier-transform infrared spectroscopy and X-ray diffraction were used to characterize the prepared nanoplatelets and nanowires. The effect of many parameters including initial concentration, pH and contact time was investigated. Values of 212.76 and 116.28 mg g^{-1} were, respectively, obtained for AlOOH-SA5 and AlOOH-SA12 for the adsorption maximum of EbT. Compared between two structures, the results indicated that the optimum conditions for 100 mg L^{-1} EbT solution were pH of 3 and 0.5 g L^{-1} AlOOH-SA5 as well as pH of 3 and 1 g L^{-1} AlOOH-SA12. Results of adsorption isotherms and adsorption kinetics indicated which they better matched by the Langmuir isotherm and also the adsorption kinetics better described by the pseudo-second-order model. Thermodynamic parameters have been measured, and results indicate that the adsorption process was spontaneous and exothermic for AlOOH-SA12 and nonspontaneous and endothermic for AlOOH-SA5. Finally, AlOOH-SA5 is a suitable adsorbent than that of AlOOH-SA12 and can be used for dye removal in wastewater treatment processes.

Keywords: Modified AlOOH; Sulfonic acid; Dye; Adsorption; Nanoplatelets; Nanowires

1. Introduction

About 70% of the worldwide market used by dyeing industries is composed of azo dyes which are synthetic dyes. A reactive azo dye contains one or more azo bonds (–N=N–) acting as chromophores in the molecular structure [1]. Also, it is the largest group of organic dyes which is challenging to degrade even at low concentrations due to its high resistance to light, heat, water and chemical and microbial attack [2]. Therefore, it is highly important to remove azo dyes from wastewater effluents before discharge into water bodies. Today, the use of adsorbents has increased for removing dyes from the wastewater [3–8].

The shape of nanoparticles is significant because a wide range of their physical and chemical properties is completely dependent on their sizes and morphologies. For example, optical or catalytic properties [9], CdTe tetrapods [10], and Cu$_2$O coated with Cu nanoparticles [11] differ depending on their morphologies. Boehmite (γ–AlOOH) and its oxide derivatives such as α–Al$_2$O$_3$ and γ–Al$_2$O$_3$ are one of these nanoscale structures receiving considerable attention, and extensive studies have been conducted on this structure for numerous uses as catalysts, adsorbents, flame retardants and optical materials [12]. Until now, several kinds of boehmite nanostructures with different physical and chemical properties such as nanorods and nanotubes

* Corresponding author.

[13], nanofibres [14] and nanowires [15] were recognized. Dyes produced by different industries are among the most hazardous materials contaminating not only water but also soil. It should also be noted that the presence of these dyes, even in very low concentrations in drinking water, causes unpleasant illnesses in humans and animals [16]. Besides, several classes of dyes are highly resistant to light, chemical and biological agents and other exposures, and their structure is not degraded. It is known that these structures cause mutations in humans [17]. Many techniques have been introduced to remove the dyes from wastewaters such as biological, oxidation or ozonation [18,19], flocculation [20], membrane separation [21] and adsorption [22–24]. From among several techniques mentioned above for the removal of dyes from water, adsorption methods are very proficient, economic, and widely used for wastewater treatment [25,26]. As a novel method for dye removal, nanostructures offer a class of promising adsorbents which are ultra-fine with a large surface area.

Therefore, in our previous work on the dye adsorption, [27–33], the purpose of this research is the synthesis and characterization of boehmite (–AlOOH) nanoplatelets and nanowires modified with sulfonic acid and the comparison between these two structures in adsorption of anionic dye in different conditions such as contact time, pH, initial anionic dye concentration and temperature. Adsorption kinetics, isothermic and thermodynamic models were considered to obtain the parameters to describe the anionic dye adsorption processes.

2. Materials and methods

In this study, a comparison between modified boehmite nanoplatelets and nanowires has been performed for dye removal from aqueous solutions. Many materials including chlorosulfonic acid, Aluminum nitrate, potassium hydroxide and sodium hydroxide with high quality were prepared of Scharlab Spanish Company (Barcelona), for the synthesis of boehmite. The Eriochrome Black T (EbT), high quality, was purchased from Merck Company.

2.1. Instruments

In this study, a Cary 100 UV–Vis spectrometer (Varian, USA) was used to study UV–Vis absorption spectra at 23°C–25°C. To measure Fourier-transform infrared spectroscopy (FTIR) spectra and X-ray powder diffraction, a Bruker spectrophotometer pressed into KBr pellets and a BRUKER B8 ADVANCE X-ray diffractometer with CuKα radiation, respectively, was used. Typically, the peaks of the adsorbent diffraction pattern in the 2θ range between 5° and 80° were scan with a velocity of 1.5°min⁻¹. A PHILIPS CM30-200 kV apparatus was used to measure transmission electron microscopy (TEM). A scanning electron microscope (Model XL30) and Metrohm 692 pH meter (Herisau, Switzerland) were used for nanoparticles size and pH measurements, respectively.

2.2. Preparation method of modified boehmite

To synthesize boehmite, we used the same method of synthesis of boehmite in the literature [28,34]. First for preparing a 0.4 M solution, 6 g of aluminium nitrate was dissolved in 40 mL of distilled water. Then sodium hydroxide (2 M), drop by drop, was added to the solution of aluminium nitrate until the observation of milky solution and the pH of the aqueous solution reaches 5, titration is stopped. The final product was put in an autoclave (100 mL) at 200°C. After 24 h, after cooling the autoclave to ambient temperature, the final deposit was separated by centrifugation apparatus. Finally using distilled water, the boehmites were washed and centrifuged in two stages and dried to achieve powder at 60°C for 24 h.

2.3. Preparation of nano-boehmite modified by SA

The SA doped boehmite was prepared through using the following method. Initially, 0.04 g of chlorosulfonic acid was added to 2 g boehmite nanoplatelets and nanowires and stirred for 5 h to form a uniform solution at room temperature. Then, the SA-boehmite was washed with distilled water several times, isolated using a centrifuge and ultimately, dried in an oven at 60°C for 2 h.

2.4. Method

For the study, the adsorption ability of EbT dye, several parameters are investigated, which include pH, temperature and time. For adsorption experiments, 0.005–0.05 g of AlOOH or AlOOH-SA was mixed with 10 mL of EbT dye solution to a suitable concentration and pH after shaking at 200 rpm and constant temperature. The pH value was adjusted between 2 and 11 using HCl (0.1 mol L⁻¹) or NaOH (0.1 mol L⁻¹) solution. Finally, using the spectrophotometer, the amount of adsorption was measured by the following equation:

$$\%\text{Removal} = \frac{C_i - C_f}{C_i} \times 100 \tag{1}$$

C_i and C_f, respectively, are the initial and final concentrations of EbT in solution. The following equivalent is then used to measure the absorption capacity:

$$q_e = \frac{C_0 - C_e}{M} \times V \tag{2}$$

In this equation, q_e is the amount of absorption capacity, and C_e and C_0, respectively, indicate the balanced and initial concentration of dye in solution (mg L⁻¹). Other parameters that are seen in the equation are V and M which indicate the solution volume (L) and dosage of the absorbance (g), respectively [35].

2.5. PZC determination

The PZC was calculated using the following method: to completely remove the CO_2 dissolved in the water, 100 mL of deionized water added to an Erlenmeyer flask which was capped with cotton and then heated for 20 min. Then, 10 mL of it was added to a 25 mL Erlenmeyer flask with 0.5 g of adsorbent and mixed for 24 h at 25°C. Finally, the

solution pH indicated the PZC. This method has been used satisfactorily [36–38].

2.6. Adsorption isotherms

The Langmuir and Freundlich are the two more common isotherms that are widely used to describe the adsorption processes. The Langmuir isotherm model is the first isotherm absorption, which is based on the molecules, or ions, bond to certain points at the surface of the adsorbent material, and monolayer absorption occurs. Besides, no interaction occurs between absorbed molecules [39]. This equation has been derived from Gibbs' method which has been shown in Eq. (3) as follows:

$$\frac{C_e}{q_e} = \frac{C_e}{q_{max}} + \frac{1}{b \times q_{max}}$$ (3)

where b (L g^{-1}) is the Langmuir constant that is related to the free energy of adsorption, q_{max} (mg g^{-1}) is the monolayer adsorption capacity, C_e (mg L^{-1}) is the adsorbate equilibrium concentration in solution and q_e (mg g^{-1}) is the concentration of adsorbate on the surface of absorber.

A dimensionless constant, R_L, known as separation factor, can be used to explain the essential characteristics of Langmuir isotherm, which is calculated using the following equation:

$$R_L = \frac{1}{(1 + bC_0)}$$ (4)

where b is the Langmuir adsorption constant (L mg^{-1}) and C_0 (mg L^{-1}) is the initial liquid phase concentration of the analyte. The value of R_L explicates the adsorption process to be linear ($R_L = 1$), unfavorable ($R_L > 1$), favorable ($0 < R_L < 1$) or irreversible ($R_L = 0$) [40].

The basis of the equilibrium Freundlich isotherm is that the absorption occurs at a heterogeneous surface that energy is not distributed uniformly. This heterogeneity leads to the creation of various functional groups on the adsorbent and, consequently, promotes the formation of various mechanisms at the interaction between absorbent and adsorbent [41]. This model is displayed as follows:

$$q_e = K_f C_e^{1/n}$$ (5)

q_e (mg g^{-1}) is the dose of dye adsorbed on the surface (mg g^{-1}), K_f is an estimated indicator of adsorption capacity. The adsorption process is favorable for $1/n$ between 0 and 1, it is difficult to carry out if $1/n \geq 2$.

2.7. Kinetic studies

To study the kinetic adsorption of adsorbents and dye, the equations of pseudo-first order (PFE) and pseudo-second order (PSE) was used. In the PFE, the intensity of adsorbent sites filling is proportional to the number of vacant sites and driving forces are considered to be linear. The PSE is based on the level of equilibrium capacity, in which the intensity of adsorbent sites filling is considered to be proportional to the square of the number of vacant sites of the adsorbent. The linear form of the PFE and PSE is shown in the following equations [42,43]:

$$\ln(q_e - q_t) = \ln q_e - k_1 t$$ (6)

$$\frac{t}{q_t} = \frac{1}{k_2 (q_e)^2} + \frac{t}{q_e}$$ (7)

q_t and q_e are the amount adsorption capacities (mg g^{-1}) and t is the time (min) at the equilibrium, and k_1 and k_2 are the first and second rate constant (L min^{-1}), respectively.

3. Results and discussion

3.1. Fourier-transform infrared spectroscopy analysis

The FTIR image of a nanoplatelets and nanowires boehmite is shown in Figs. 1a and 2a. Peaks in 730.3; 1,070.83; 1,151; 2,090.13; 3,080.01; and 3,272.52 cm^{-1} indicate the structure of nanoplatelets and nanowires boehmite [27]. Also, the peak in 3,080.01 and 3,272.52 cm^{-1} related to –OH and Al–O, respectively. Figs. 1b and 2b are related to the nano–AlOOH modified with sulfonic acid, which is very similar to Figs. 1a and 2a; however, compared with the previous figure, a series of peaks have been added in areas; 1,649.25 (1,644.93) cm^{-1} and 2,964 cm^{-1} relate to S=O groups and OH stretching absorption of the SO$_3$H group, respectively. The results of this section confirm that the sulfonic groups have functionalized the surface of the nano-AlOOH.
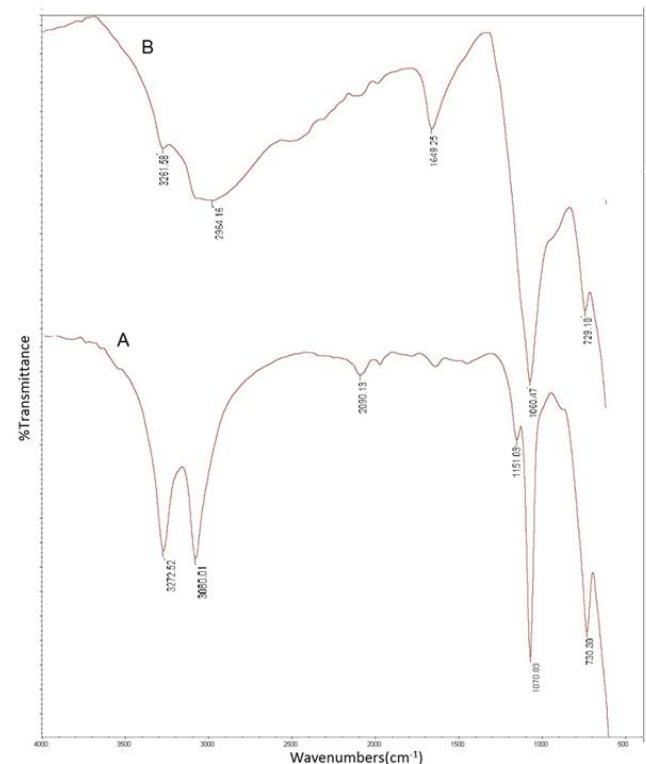

Fig. 1. FTIR image of (a) AlOOH and (b) AlOOH-SA12 adsorbents.
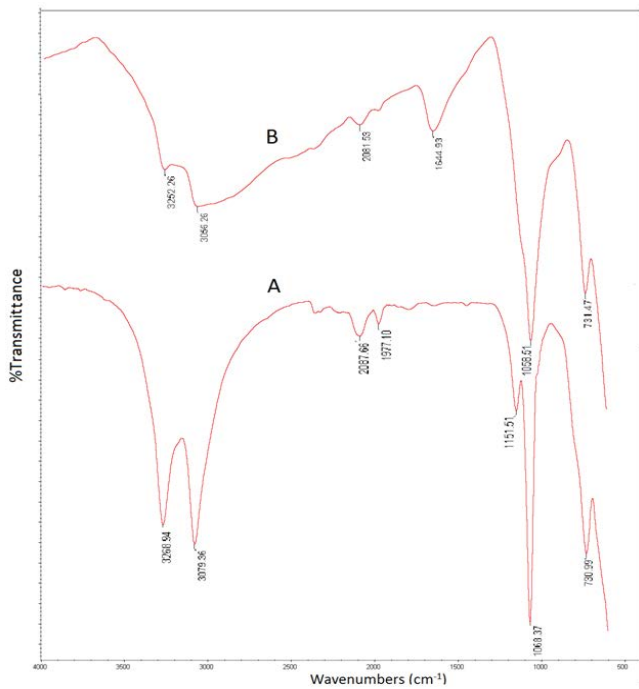
Fig. 2. FTIR image of (a) AlOOH and (b) AlOOH-SA5 adsorbents.

3.2. Analysis of SEM, TEM and X-ray diffraction

The images of scanning electron microscopy (SEM) and transmission electron microscopy (TEM) related to the nano-boehmite are shown in Fig. 3. The AlOOH12 structure constructed in the alkali pH was plate-shaped, with the nanoscale size of about 50 nm. The structure of AlOOH5 constructed in the acidic pH was rod-shaped with nanoscale size. As the figures show, the length and height of the particles were about 50 and 100 nm, respectively.

Findings of the X-ray diffraction (XRD) test for two samples of nano-AlOOH and nano- AlOOH modified with sulfonic acid are shown in Figs. 4 and 5. Compared with the standard cards, nanoparticles, or nano-adsorbents, are well synthesized because the sample peaks are similar to the standard sample. Findings of the XRD test for the AlOOH-SA and its comparison with the standard sample suggested that the structure of the nano-boehmite remained fixed after the modification of its surface, showing no change.

The initial peak that highly increased indicates the anisotropic crystallographic nature of the particles in the sample of AlOOH-SA5, in which no impure peak is observed. However, in the sample of AlOOH-SA12, impurities are observed in the structure. Finally, using the Schwartz equation, the mean particle size was obtained as 22.90 nm for the AlOOH-SA5 and 17.81 nm for the AlOOH-SA12.
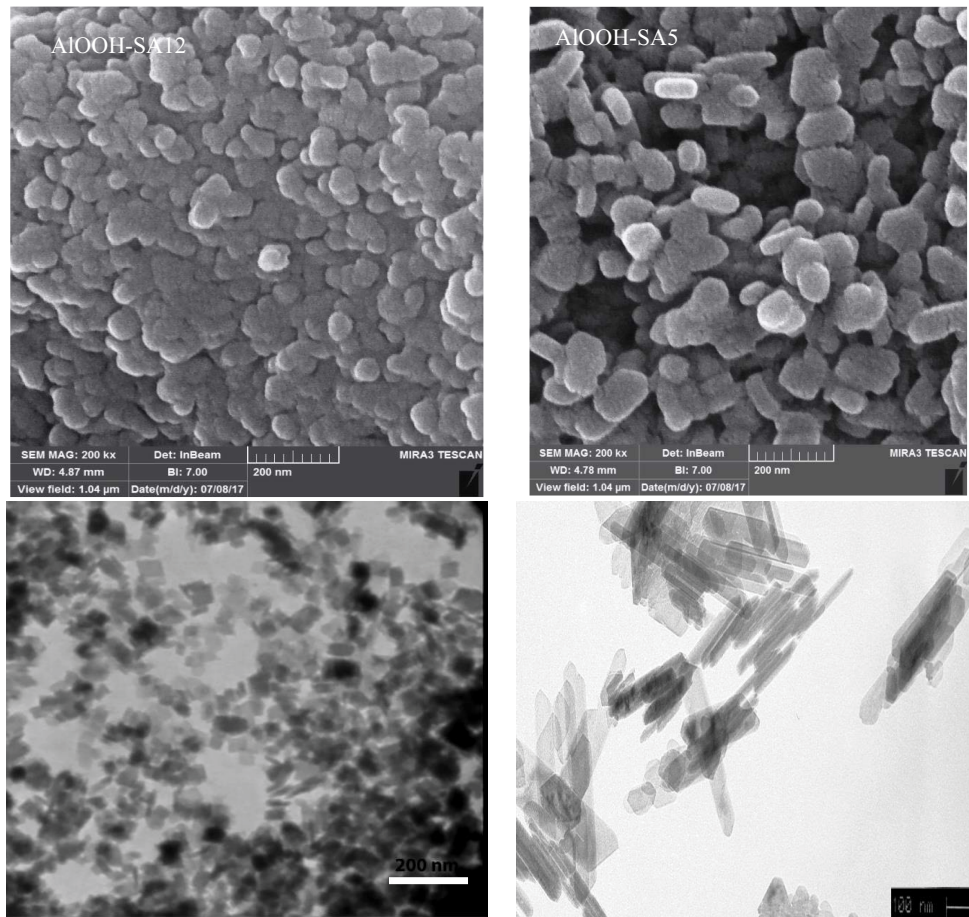

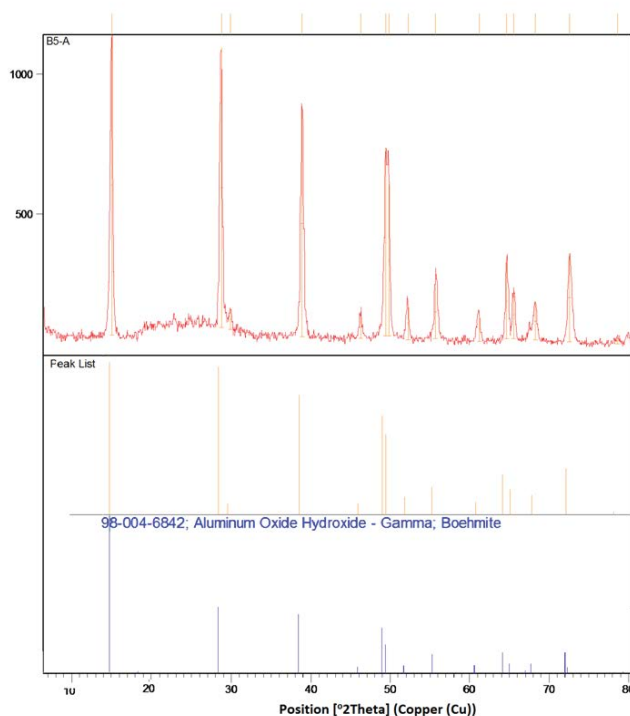Fig. 3. SEM and TEM images of AlOOH adsorbents.
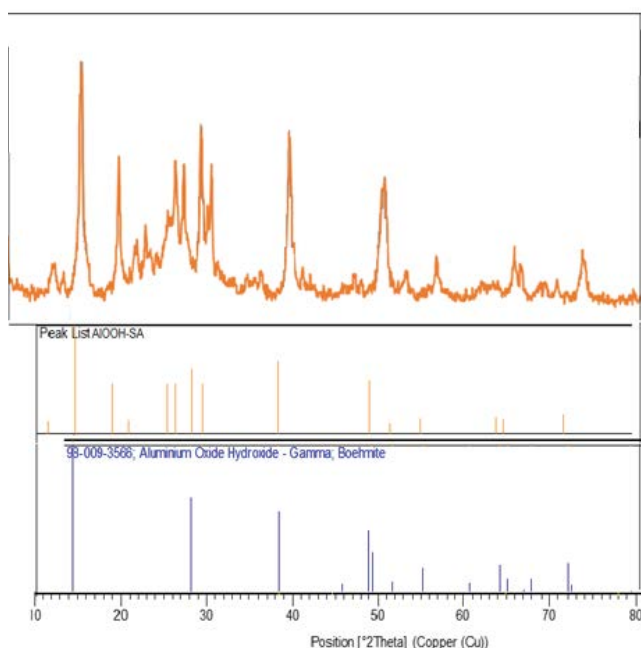
Fig. 4. XRD image of AlOOH-SA5 adsorbent.

Fig. 5. XRD images of AlOOH and AlOOH-SA12 adsorbents.

3.3. Studying the pH effect on the removal efficiency

One of the key factors on the general adsorption process is the effect of pH, which affects the chemical properties of both adsorbents and dyes in solution. To study the effect of pH on the adsorption process, 0.03 g of AlOOH-SA5 and AlOOH-SA12 were added to 10 mL and 100 ppm of EbT solution and the pH of the solution was set at 2–11.
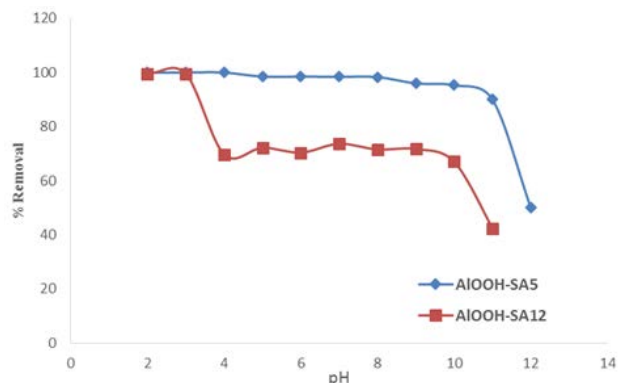

Fig. 6. Effect of pH on adsorption of EbT dye on the adsorbents (conditions: 30 mg adsorbent, 10 mL of 100 mg L^{-1} of dye, duration of oscillation time of 20 min).

Fig. 6 clearly shows the dependence of pH on the EbT adsorption efficiency onto the adsorbents.

For the AlOOH-SA5 adsorbent, however, with increasing of the pH, the removal amount of EbT is constant when the pH value <11 and, thus, pH = 3 was selected as the best pH. For the AlOOH-SA12 adsorbent, with the increase of pH, the EbT removal rate stayed constant up to pH = 3 and then, decreased with increasing the pH value. For this adsorbent, pH = 3 was the best pH in removing the EbT dye. At lower pH values (pH < pH$_{PZC}$), the adsorbent had a positive charge. Moreover, the EbT dye may be present in anionic forms. In such conditions, EbT molecules have high tendency with it. By increasing the pH value (pH ≥ pH$_{PZC}$), it tends to change in inverse [44,45].

The PZC of the AlOOH-SA5 and AlOOH-SA12 are 1.65 and 1.75, respectively, the forming of a negative charge on the adsorbent surface is easy, then the dye contains a negative charge will combine with adsorbent [46]. Thus, the boehmite adsorbed anionic dyes, and the solution pH was lower than the pH$_{PZC}$ of AlOOH, which was beneficial for the adsorption.

3.4. Effect of adsorbent dosage and contact time on the dye removal

To examine the effect of adsorbent dosage on dye removal, different dosages of the adsorbent were used for the adsorption of the 100 ppm EbT solution. Results in Fig. 7 are shown that by increasing the adsorbent dosage from 0.02 to 0.03 g led to an increase of the dye removal rate, whereas its increase from 0.03 to 0.06 g was accompanied with the decreased dye removal rate. The obtained optimal mass for the AlOOH-SA5 adsorbent was equal to 0.005 g. Similar results were obtained for AlOOH-SA12 where the optimal mass for the adsorbent was measured as 0.01 g. The capacity of dye adsorption generally increases with increasing absorbent dosage because the increased dosage of the adsorbent is associated with increased special surface and adsorption sites [47,48].

Results of Fig. 8 show that removal efficiency increases with increasing the contact time and reaches the optimum at 20 min for AlOOH-SA5 and 30 min for AlOOH-SA12.

The removal percentage also reaches 100% and 99.5%, respectively. After this, increase in adsorption was very less, because of the availability and abundance of empty sites on the surface of the adsorbent, the rapid adsorption of EbT happens in the first few minutes.

3.5. Studying the initial dye concentration

Fig. 9 shows the effect of EbT dye concentration on the surface. To study this test, several parameters such as time,
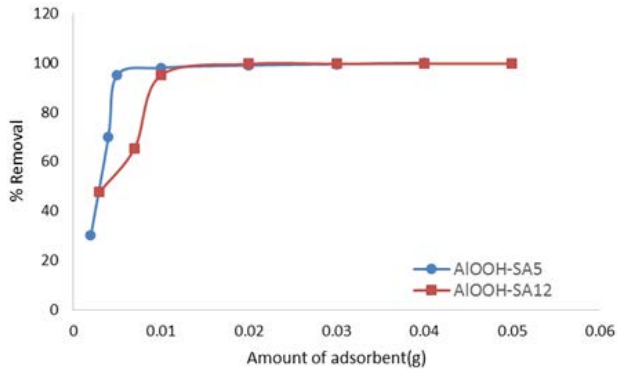

Fig. 7. Effect of adsorbent weight on adsorption of dye on the adsorbents (conditions: 10 mL of 100 mg L^{-1} of EbT, duration of oscillation time of 20 min).
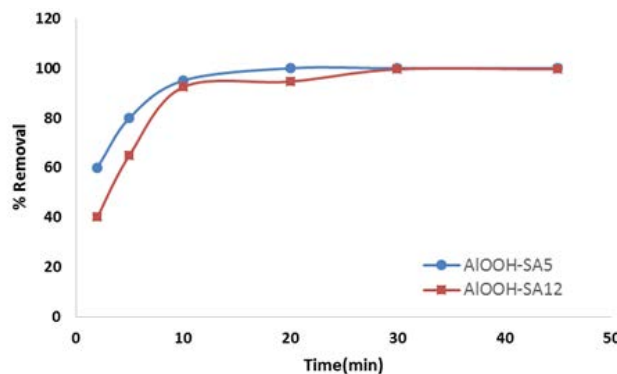

Fig. 8. Effect of reaction time on adsorption of EbT on the adsorbents (conditions: 10 mL of 100 mg L^{-1} of EbT).
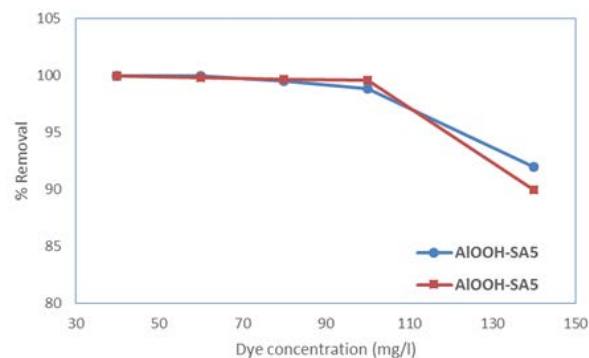

Fig. 9. Effect of initial dye concentration on adsorption of EbT dye.

dosage of adsorbent and pH were regulated on the optimum values and the adsorption dye investigated at different concentrations. According to this figure, when the initial dye concentration increases, the amount of the adsorbed dye is reduced. It can be concluded that dye removal is affected by its initial concentration.

However, at low concentrations of dye, it is possible that empty spots or active sites are more accessible on the absorbent surface than when there is a high concentration of EbT in the solution. Alternatively, with the increase in EbT concentration, the number of EbT molecules is also increased, so there are fewer active sites on the absorbent surface. Therefore, available active sites are quickly saturated and the percentage of dye removal decreased.

3.6. Comparing the amount of adsorption of EbT by the AlOOH-SA5 and AlOOH-SA12 by AlOOH5 and AlOOH12

By comparing the different adsorbents, the adsorption capacity of the EbT significantly increases if the modified adsorbents were used as the adsorbent.

In brief, the purposes behind using AlOOH modified by SA were:

- Increasing the amount of adsorption of EbT
- Decreasing the time of reaction
- Decreasing the amount of adsorbent

The information presented in Table 1 displays the results of adsorption capacity of different adsorbents for removing EbT from the solution.

3.7. Results of the adsorption isotherms and kinetics

Fig. 10 presents the adsorption isotherm of AlOOH-SA5/AlOOH-SA12 for EbT dye which it was fitted based on the adsorption process data. Table 2 presents the correlation coefficients and the adsorbent parameters. As shown in Table 2, the Langmuir model well fitted the adsorption isotherms, and theoretically, absorption capacity has the highest amount [33,48].

The EbT dye adsorption on the adsorbents carries out quickly, as is inferred from the values of $1/n$ and R_L obtained from the Langmuir and Freundlich models, respectively; however, the dye adsorption carries out favourable. By considering the results of this section, we can conclude that there is monolayer adsorption for the EbT dye on the adsorbents.

Kinetic models can be used as an appropriate model that has information to understand the absorption mechanisms. The most widely used equations are the pseudo-first and

Table 1
Effect of different adsorbent on adsorption capacity (initial dye concentration of 100 mg L^{-1} and optimum condition)

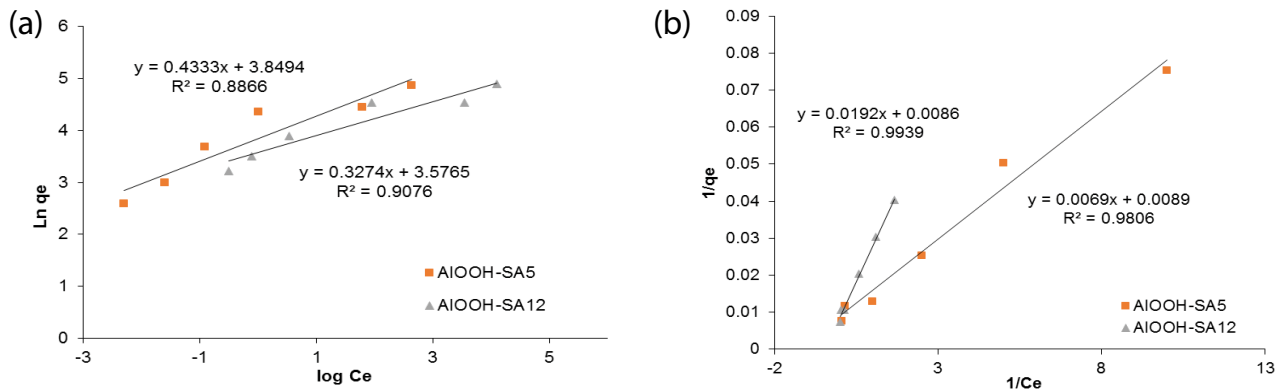| Adsorbent	q_{max} (mg g^{-1})
AlOOH5	111.11
AlOOH-SA5	221.76
AlOOH12	38.40
AlOOH-SA12	116.28

Fig. 10. Adsorption isotherms of dye adsorbed onto AlOOH-SA in aqueous solution; Langmuir model (a) and Freundlich model (b).

Table 2
Comparison of dyes adsorption capacity of different adsorbents

Adsorption isotherm		AlOOH-SA5	AlOOH-SA12
Langmuir equation	R^2	**0.984**	**0.9939**
	q_{max} (mg g^{-1})	**212.76**	**116.28**
	K_L (L mg^{-1})	0.376	4.48
	R_L	0.026	0.0022
Freundlich equation	R^2	**0.790**	**0.907**
	K_F (mg g^{-1})	59.07	35.51
	$1/n$	0.42	0.327

second-order models. The PSE and PFE models were used to study the adsorption kinetics of the EbT dye by adsorbents.

According to Fig. 11, the PSE model was fitted best to the experimental data which indicates that the rate-limiting step is the chemical absorption that involves electron transfer between the absorbent and adsorbate by the valence force [8,33]. The constants of k_1 and k_2 are shown in Table 3.

3.8. Adsorption mechanism research

Adsorption, by regarding the theory of classical physical chemistry, is a surface effect. Due to the different nature of the interaction between adsorbent and adsorbate, it is divided into two parts, physical and chemical adsorption [49]. The Van der Waals, VDW, forces are the main interaction for physical adsorption. Because there is no chemical bonds produce between the adsorbents and anionic dye, so
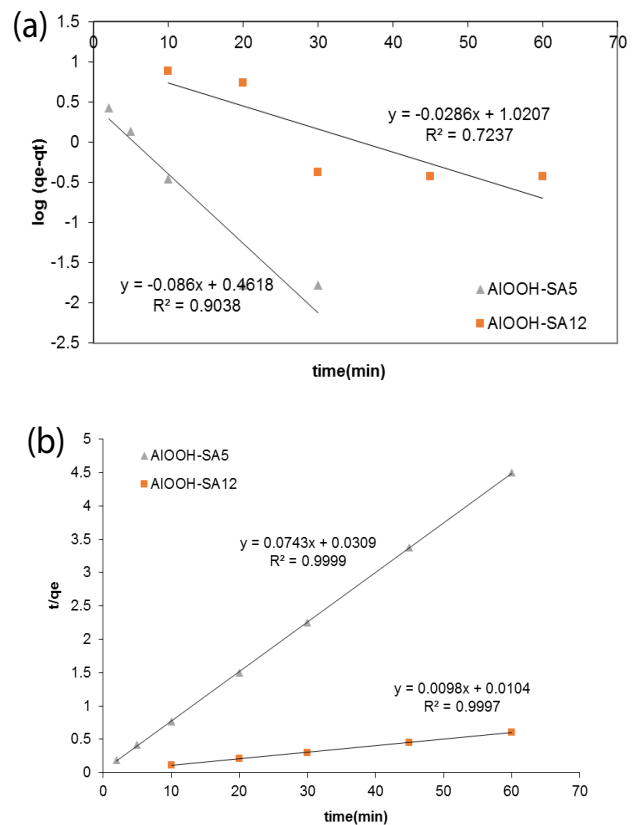
Fig. 11. Kinetic models for the adsorption of dyes; pseudo-first-order (a) and pseudo-second-order (b) kinetics.

Table 3
Pseudo-first-order and pseudo-second-order model parameters constants for the adsorption of dyes on AlOOH-SA5 and AlOOH-SA12

Absorbents	PFE model			PFE model		
	k_1 (min^{-1})	q_e (mg g^{-1})	R^2	q_e (mg g^{-1})	k_2 (g mg^{-1} min^{-1})	R^2
AlOOH-SA5	0.0483	11.298	0.863	33.89	0.029	0.9997
AlOOH-SA-12	0.0286	10.47	0.723	102.04	0.0092	0.9997

the adsorption process is the physical absorption. The possible forms of the physical adsorption process are hydrogen bonds, π-π effect, electrostatic effect and VDW etc. There are numerous factors such as the steric hindrance intensity of the adsorbate, electric intensity of the hydrogen bond donor and acceptor, and the electrostatic effect which affect the physical adsorption process.

Fig. 12 presents the structure and related properties of the EbT dye. The results present that the AlOOH-SA has many sulfonyl and hydroxyl groups onto the surface; a hydrogen bond will be formed by combining these groups with adsorbate and between them.

By studying the dye, it can be realized that the sulfonyl group of EbT, with electron donor and receptor, is easy to combine with adsorbent and formed hydrogen bond [50]. The adsorption effect, in the EbT solution, mainly depends on hydrogen bonds, because of the existence of electronic donors and receptor, the formation of the hydrogen bond is easy. Therefore, AlOOH-SA combines with a large number of sulfonyl groups easily [50].

The structure of synthesized boehmite at pH of 5 is exfoliated (1D), but at pH of 12 it is platelet-like (2D), and in the exfoliated structure, the number of activated sites is higher than the platelet-like structure. Therefore, the adsorption of EbT dye in AlOOH5 adsorbent is more than the AlOOH12 adsorbent [51,52].

3.9. Thermodynamic studies

The changes of enthalpy ($\Delta H°$), Gibb's free energy ($\Delta G°$) and entropy ($\Delta S°$) for the adsorption were determined by the following equations:

$$\ln K_l = \frac{\Delta S°}{R} - \frac{\Delta H°}{RT} \tag{8}$$

$$\Delta G° = \Delta H° - T\Delta S° \tag{9}$$

where T is the solution temperature (K), R is the universal gas constant (8.314 J K^{-1} mol^{-1}) and K_l is the equilibrium constant [53]. The calculated parameters of thermodynamics are demonstrated in Table 4.

The values of Gibbs free energy $\Delta G°$ were calculated by knowing the $\Delta H°$ and $\Delta S°$, and $\Delta H°$ was obtained from the plot of ln K_l vs. $1/T$ from Eq. (8). Once these two parameters were obtained, $\Delta G°$ was determined from Eq. (9). The
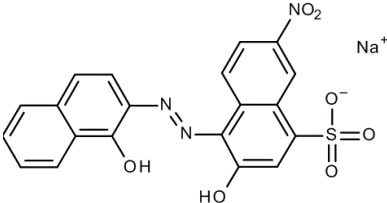
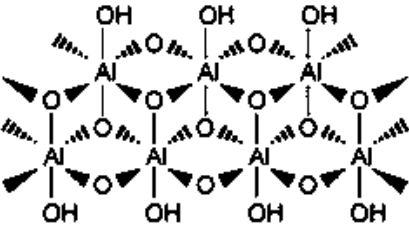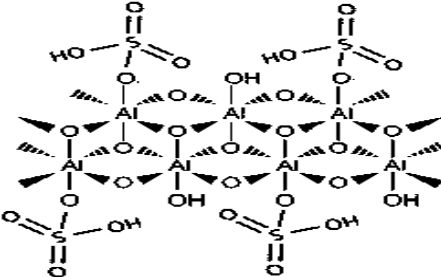| Dyes and adsorbent	Structural formula	Molecular formula	Molecular weight (g/moL)
EbT		$C_{28}H_{31}ClN_2O_3$	479.017
AlOOH			
AlOOH-SA			

Fig. 12. Structure and properties of cationic dyes and adsorbents.

Table 4
Thermodynamic parameters for the adsorption of adsorbents at different temperatures

| | | | ΔG° (kJ mol^{-1}) | | |
| | | | T (ºC) | | |
	ΔS° (kJ mol^{-1})	ΔH° (kJ mol^{-1})	20	40	60
AlOOH-SA5	−0.0595	15.041	32.47	33.66	34.55
AlOOH-SA12	0.0006	−2.165	−2.341	−2.353	−2.362

increased randomness at the solid/solution interface during the adsorption occurs when the value of ΔS° is positive [54,55]. The negative values of ΔG° in Table 4 for AlOOH-SA12 reveal that Ebt dye adsorption by adsorbents is a spontaneous process. Also, it is considered that the ΔG° values decreased with temperature growth from 20°C to 60°C, indicating that the process was more efficient at the higher temperature. Furthermore, the ΔG° of less than −15 kJ mol^{-1} implies that the interactions between metal ions and adsorbent sites are physical. Moreover, according to Table 3 for dye adsorption by adsorbents, the positive value of ΔS° and negative value of ΔH° represent that the process is exothermic with increase in randomness at the solid–solution interface within adsorption [56]. The lower adsorption heat obtained in this work indicated that physical rather than the chemisorption was prevailing [57]. The result obtained for AlOOH-SA6 shows that the change of activation ΔG is positive and it suggests that adsorption process for converting reactants into products requires energy. The ΔG value determines the reaction rate, rate increases as ΔG decreases, and hence the energy requirement is fulfilled, the reaction proceeds. The endothermic process happens when the value of ΔH is positive, which means that the reaction consumes energy. The negative ΔS value indicates that the adsorption leads to order through the formation of activated complex suggesting that dye adsorption adsorbent surface is an associated mechanism. Also when the amount of ΔS is negative, it usually means that no significant change occurs in the internal structure of the adsorbent during the adsorption process [33,58].

4. Conclusion

In this study, the ability of EbT removal from aqueous solutions was examined by two structures of boehmite (nanoplatelets and nanowires) modified by sulfonic acid, and these structures were characterized by XRD, SEM, TEM and FTIR. The results of TEM and SEM indicated that the AlOOH-SA12 structure is plate-shaped and the structure of AlOOH-SA5 is rod-shaped. The results indicated that the optimum conditions for 100 mg L^{-1} EbT solution were pH of 3 and 0.5 g L^{-1} AlOOH-SA5 as well as pH of 3 and 1 g L^{-1} AlOOH-SA12. Also, the study of the AlOOH-SA5 and AlOOH-SA12 adsorption capability revealed that there are many factors affected on them such as hydrogen bond, pH, electrostatic effect and materials structure. In summary, we presented comparative adsorption of two structure of boehmite (nanoplatelets and nanowires) modified by sulfonic acid adsorbents; the adsorption capability of AlOOH-SA5 was better than that of AlOOH-SA12. Boehmite as an alternative adsorbent can be used for dye removal in wastewater treatment processes in the future environment governance.

References

[1] A.A. Ahmad, B.H. Hameed, Fixed-bed adsorption of reactive azo dye onto granular activated carbon prepared from waste, J. Hazard. Mater., 175 (2010) 298–303.
[2] Ö. Gerçel, H.F. Gerçel, A.S. Koparal, Ü.B. Öğütveren, Removal of disperse dye from aqueous solution by novel adsorbent prepared from biomass plant material, J. Hazard. Mater., 160 (2008) 668–674.
[3] A. Naghizadeh, M. Kamranifar, A.R. Yari, M.J. Mohammadi, Equilibrium and kinetics study of reactive dyes removal from aqueous solutions by bentonite nanoparticles, Desal. Wat. Treat., 97 (2017) 329–337.
[4] G. Zeydouni, M. Kianizadeh, Y. Omidi Khaniabadi, H. Nourmoradi, S. Esmaeili, M.J. Mohammadi, R. Rashidi, Eriochrme black-T removal from aqueous environment by surfactant modified clay: equilibrium, kinetic, isotherm, and thermodynamic studies, Toxin Rev., (2018) 1–11, Available at: https://doi.org/10.1080/15569543.2018.1455214..
[5] H. Biglari, S. RodríguezíCouto, Y.O. Khaniabadi, H. Nourmoradi, M. Khoshgoftar, A. Amrane, M. Vosoughi, S. Esmaeili, R. Heydari, M.J. Mohammadi, Cationic surfactant-modified clay as an adsorbent for the removal of synthetic dyes from aqueous solutions, Int. J. Biol. Macromol., 16 (2018) 1–11.
[6] Y. Khaniabadi, H. Basiri, H. Nourmoradi, M. Mohammadi, A. R. Yari, S. Sadeghi, A. Amrane, Adsorption of Congo Red dye from aqueous solutions by montmorillonite as a low-cost adsorbent, Int. J. Chem. React. Eng., 16 (2018) 11.
[7] H. Rezaei, M.R. Narooie, R. Khosravi, M.J. Mohammadi, H. Sharafi, H. Biglari, Humic acid removal by electrocoagulation process from natural aqueous environments, Int. J. Electrochem. Sci., 13 (2018) 2379–2389.
[8] F. Salimi, H. Rahimi, C. Karami, Removal of methylene blue from water solution by modified nanogoethite by Cu, Desal. Wat. Treat., 137 (2019) 334–344.
[9] R. Si, Y.-W. Zhang, L.-P. You, C.-H. Yan, Rare-earth oxide nanopolyhedra, nanoplates, and nanodisks, Angewandte Chemie, 117 (2005) 3320–3324.
[10] L. Manna, D.J. Milliron, A. Meisel, E.C. Scher, A.P. Alivisatos, Controlled growth of tetrapod-branched inorganic nanocrystals, Nature Mat., 2 (2003) 382–385.
[11] S.U. Son, I.K. Park, J. Park, T. Hyeon, Synthesis of Cu₂O coated Cu nanoparticles and their successful applications to Ullmann-type amination coupling reactions of aryl chlorides, Chem. Commun., (2004) 778–779.
[12] D. Mishra, S. Anand, R.K. Panda, R.P. Das, Hydrothermal preparation and characterization of boehmites, Mater. Lett., 42 (2000) 38–45.

[13] H. Hou, Y. Xie, Q. Yang, Q. Guo, C. Tan, Preparation and characterization of γ-AlOOH nanotubes and nanorods, Nanotechnology, 16 (2005) 741.

[14] A. Wierenga, A.P. Philipse, H.N. Lekkerkerker, D.V. Boger, Aqueous dispersions of colloidal boehmite: structure, dynamics, and yield stress of rod gels, Langmuir, 14 (1998) 55–65.

[15] J. Zhang, S. Liu, J. Lin, H. Song, J. Luo, E. Elssfah, E. Ammar, Y. Huang, X. Ding, J. Gao, Self-assembly of flowerlike AlOOH (boehmite) 3D nanoarchitectures, J. Phys. Chem. C, 110 (2006) 14249–14252.

[16] L. Ai, C. Zhang, F. Liao, Y. Wang, M. Li, L. Meng, J. Jiang, Removal of methylene blue from aqueous solution with magnetite loaded multi-wall carbon nanotube: kinetic, isotherm and mechanism analysis, J. Hazard. Mater., 198 (2011) 282–290.

[17] G. Crini, Non-conventional low-cost adsorbents for dye removal: a review, Bioresour. Technol., 97 (2006) 1061–1085.

[18] P. Malik, S. Saha, Oxidation of direct dyes with hydrogen peroxide using ferrous ion as catalyst, Sep. Purif. Technol., 31 (2003) 241–250.

[19] M. Koch, A. Yediler, D. Lienert, G. Insel, A. Kettrup, Ozonation of hydrolyzed azo dye reactive yellow 84 (CI), Chemosphere, 46 (2002) 109–113.

[20] T. Panswad, S. Wongchaisuwan, Mechanisms of dye waste-water colour removal by magnesium carbonate-hydrated basic, Water Sci. Tech., 18 (1986) 139–144.

[21] G. Ciardelli, L. Corsi, M. Marcucci, Membrane separation for wastewater reuse in the textile industry, Resour., Conserv. Recycl., 31 (2001) 189–197.

[22] N. Thinakaran, P. Baskaralingam, M. Pulikesi, P. Panneerselvam, S. Sivanesan, Removal of Acid Violet 17 from aqueous solutions by adsorption onto activated carbon prepared from sunflower seed hull, J. Hazard. Mater., 151 (2008) 316–322.

[23] M. Anbia, S.E. Moradi, Adsorption of naphthalene-derived compounds from water by chemically oxidized nanoporous carbon, Chem. Eng. J., 148 (2009) 452–458.

[24] M. Anbia, K. Mohammadi, Novel and efficient nanoporous adsorbent for dichromate ion and furfural removal from aqueous solutions, Asian J. Chem, 21 (2009) 3347–3354.

[25] A. Namane, A. Mekarzia, K. Benrachedi, N. Belhaneche-Bensemra, A. Hellal, Determination of the adsorption capacity of activated carbon made from coffee grounds by chemical activation with $ZnCl_2$ and H_3PO_4, J. Hazard. Mater., 119 (2005) 189–194.

[26] M. Kaykhaii, M. Sasani, S. Marghzari, Removal of dyes from the environment by adsorption process, Chem. Mater. Eng., 6 (2018) 31–35.

[27] F. Salimi, M. Abdollahifar, P. Jafari, M. Hidaryan, A new approach to synthesis and growth of nanocrystalline AlOOH with high pore volume, J. Serb. Chem. Soc., 82 (2017) 203–213.

[28] F. Salimi, M. Abdollahifar, A.R. Karami-gazafi, The effect of NaOH and KOH on the characterization of mesoporous AlOOH in the Solvothermal route, Ceramics Silikáty, 60 (2016) 273–277.

[29] F. Salimi, S.S. Emami, C. Karami, Removal of methylene blue from water solution by modified nano-boehmite with Bismuth, Inorg. Nano-Met. Chem., 48 (2018) 31–40.

[30] F. Salimi, M. Eskandari, C. Karami, Investigating of the methylene blue adsorption of wastewater using modified nano-zeolite by copper, Desal. Wat. Treat., 85 (2017) 206–214.

[31] F. Salimi, K. Tahmasobi, C. Karami, A. Jahangiri, Preparation of modified nano-SiO_2 by bismuth and iron as a novel remover of methylene blue from water solution, J. Mex. Chem. Soc., 61 (2017) 250–259.

[32] M. Mohamadi, F. Salimi, S. Sadeghi, Reduction of oil, COD and turbidity of Kermanshah oil refinery effluent using modified nano-zeolite by bismuth and iron, Desal. Wat. Treat., 97 (2017) 151–157.

[33] J. Rezaee, F. Salimi, C. Karami, Removal of eriochrome black T dye from water solution using modified nano-boehmite by organic compounds, Desal. Wat. Treat., 139 (2019) 342–351.

[34] N. Haghnazari, M. Abdollahifar, F. Jahani, The Effect of NaOH and KOH on the characterization of mesoporous AlOOH

[35] L. Cui, Y. Wang, L. Gao, L. Hu, L. Yan, Q. Wei, B. Du, EDTA functionalized magnetic graphene oxide for removal of Pb (II), Hg (II) and Cu (II) in water treatment: adsorption mechanism and separation property, Chem. Eng. J., 281 (2015) 1–10.

[36] X. Deng, L. Lü, H. Li, F. Luo, The adsorption properties of Pb (II) and Cd (II) on functionalized graphene prepared by electrolysis method, J. Hazard. Mater., 183 (2010) 923–930.

[37] R. Leyva-Ramos, L. Bernal-Jacome, I. Acosta-Rodriguez, Adsorption of cadmium (II) from aqueous solution on natural and oxidized corncob, Sep. Purif. Technol., 45 (2005) 41–49.

[38] C. Moreno-Castilla, M. Lopez-Ramon, F. Carrasco-Marın, Changes in surface chemistry of activated carbons by wet oxidation, Carbon, 38 (2000) 1995–2001.

[39] Y. Liu, X. Li, Z. Xu, Z. Hu, Preparation of flower-like and rod-like boehmite via a hydrothermal route in a buffer solution, J. Phys. Chem. solids, 71 (2010) 206–209.

[40] S.Z. Ali, M. Athar, M. Salman, M.I. Din, Simultaneous removal of Pb (II), Cd (II) and Cu (II) from aqueous solutions by adsorption on triticum aestivum-a green approach, Hydrology: Current Res., 2011 (2012)

[41] J.-Z. Guo, B. Li, L. Liu, K. Lv, Removal of methylene blue from aqueous solutions by chemically modified bamboo, Chemosphere, 111 (2014) 225–231.

[42] A.K. Meena, G.K. Mishra, P.K. Rai, C. Rajagopal, P.N. Nagar, Removal of heavy metal ions from aqueous solutions using carbon aerogel as an adsorbent, J. Hazard. Mater., 122 (2005) 161–170.

[43] Y. Hamzeh, A. Ashori, E. Azadeh, A. Abdulkhani, Removal of Acid Orange 7 and Remazol Black 5 reactive dyes from aqueous solutions using a novel biosorbent, Mater. Sci. Eng.: C, 32 (2012) 1394–1400.

[44] M. Heidari-Chaleshtori, A. Nezamzadeh-Ejhieh, Clinoptilolite nano-particles modified with aspartic acid for removal of Cu (II) from aqueous solutions: isotherms and kinetic aspects, New J. Chem., 39 (2015) 9396–9406.

[45] E. Shabani, F. Salimi, A. Jahangiri, Removal of Arsenic and Copper from Water Solution Using Magnetic Iron/Bentonite Nanoparticles (Fe_3O_4/Bentonite), Silicon, 11 (2018) 961–971.

[46] M. Kosmulski, pH-dependent surface charging and points of zero charge II. Update, J. Colloid Interface Sci., 275 (2004) 214–224.

[47] B. Tanhaei, A. Ayati, M. Sillanpää, Magnetic xanthate modified chitosan as an emerging adsorbent for cationic azo dyes removal: kinetic, thermodynamic and isothermal studies, Int. J. Biol. Macromol., 121 (2019) 1126–1134.

[48] M. Shahadat, S.F. Azha, S. Ismail, Z. Shaikh, S.A. Wazed, Treatment of Industrial Dyes Using Chitosan-Supported Nanocomposite Adsorbents, In: The Impact and Prospects of Green Chemistry for Textile Technology, Elsevier, 2019, 509–539.

[49] N. Saad, M. Al-Mawla, E. Moubarak, M. Al-Ghoul, H. El-Rassy, Surface-functionalized silica aerogels and alcogels for methylene blue adsorption, RSC Advances, 5 (2015) 6111–6122.

[50] H. Han, W. Wei, Z. Jiang, J. Lu, J. Zhu, J. Xie, Removal of cationic dyes from aqueous solution by adsorption onto hydrophobic/hydrophilic silica aerogel, Colloids Surf. A, 509 (2016) 539–549.

[51] C. Xiang Ying, H. Hyun Sue, W.L. Soon, Hydrothermal synthesis of boehmite (γ-AlOOH) nanoplatelets and nano-wires: pH-controlled morphologies, Nanotechnology, 18 (2007) 285608.

[52] Q. Liang, X. Guo, T. Quan, F. Meng, P123 assisted synthesis and characterization of urchin-like γ-Al_2O_3 hollow micro-spheres, J. Adv. Ceram., 5 (2016) 225–231.

[53] B.S. Inbaraj, J.S. Wang, J.F. Lu, F.Y. Siao, B.H. Chen, Adsorption of toxic mercury (II) by an extracellular biopolymer poly (γ-glutamic acid), Bioresour. Technol., 100 (2009) 200–207.

[54] V.S. Mane, I.D. Mall, V.C. Srivastava, Kinetic and equilibrium isotherm studies for the adsorptive removal of Brilliant Green dye from aqueous solution by rice husk ash, J. Environ. Manage., 84 (2007) 390–400.

[55] P. Pimentel, M.A.F. Melo, D.M.A. Melo, A.L.C. Assuncao, D.M. Henrique, C.N. Silva Jr, G. Gonzalez, Kinetics and thermodynamics of Cu (II) adsorption on oil shale wastes, Fuel Process. Technol., 89 (2008) 62–67.

[56] G. Sheng, J. Li, D. Shao, J. Hu, C. Chen, Y. Chen, X. Wang, Adsorption of copper (II) on multiwalled carbon nanotubes in the absence and presence of humic or fulvic acids, J. Hazard. Mater., 178 (2010) 333–340.

[57] G. McKay, Use of Adsorbents for the Removal of Pollutants from Wastewater, CRC press, Boca Raton, 1995.

[58] M. Doğan, H. Abak, M. Alkan, Adsorption of methylene blue onto hazelnut shell: kinetics, mechanism and activation parameters, J. Hazard. Mater., 164 (2009) 172–181.